

INVITED PAPER – SPECIAL SESSION ON “SIGNAL PROCESSING FOR RADAR IMAGING”

OPTIMISED IMAGE AUTOFOCUSING FOR POLARIMETRIC ISAR

Marco Martorella¹, L. Cantini², F. Berizzi¹, B. Haywood³, E. Dalle Mese¹

¹ Dept. of “Ingegneria dell’Informazione”, via Caruso 16, 56123 Pisa – Italy

² ISL, Ingegneria dei Sistemi Logistici, ALTRAN Group, via di Marmiceto 6/C, 56121 Loc. Ospedaletto, Pisa – Italy

³ Defence Science & Technology Organisation, PO Box 1500, Edinburgh, SA 5111 – Australia

ABSTRACT

The use of full polarisation enables multi-channel SAR processing for enhancing both imaging and classification capabilities. In the field of Inverse Synthetic Aperture Radar (ISAR) very little has been investigated, especially from the point of view of multi-channel ISAR image formation. In this paper, the authors want to define an optimised image autofocusing technique that exploits full polarisation information. Theory and simulation results will be provided in the paper.

1. INTRODUCTION

Fully polarimetric radars have been widely exploited for improving detection and classification performance [1],[2]. In addition, fully polarimetric Synthetic Aperture Radar (SAR) systems have been introduced to enable new applications in radar imaging [3],[4]. In the ISAR field, the information associated with the signal polarisation can be exploited for enhancing target classification capabilities. The advantages come from: 1) additional information associated with scattering mechanisms (and therefore with scattering centre shapes) and 2) better ISAR image formation. In particular, ISAR image focusing takes advantage from a fully polarimetric radar.

The goals of this paper are: 1) to derive a mathematical formulation of the ISAR image autofocusing problem when using polarimetric data, 2) to define an algorithm for ISAR image autofocusing for fully polarimetric data, and 3) to prove its effectiveness when compared to single polarisation ISAR processing.

2. MATHEMATICAL ASPECTS OF SIGNAL MODELLING AND ISAR PROCESSING FOR POLARIMETRIC DATA

In this section a new framework for ISAR imaging will be provided by introducing polarimetric ISAR processing.

2.1 Signal Model

The polarimetric matrix of the received signal, in free space conditions, can be written in a time-frequency domain by extending the signal model defined in [5]:

$$\mathbf{S}_R(f, t) = W(f, t) e^{-j\frac{4\mathbf{p}f}{c}R_0(t)} \cdot \int_V \mathbf{z}(z) \exp\left\{-j\frac{4\mathbf{p}f}{c}\left[\mathbf{z}^T \cdot \mathbf{i}_{R_0}(t)\right]\right\} dz + \mathbf{N}(f, t) \quad (1)$$

The polarimetric matrix of the received signal can be expressed as $\mathbf{S}_R(f, t) = \begin{bmatrix} S_R^{HH}(f, t) & S_R^{HV}(f, t) \\ S_R^{VH}(f, t) & S_R^{VV}(f, t) \end{bmatrix}$. In eq. (1)

$W(f, t) = \text{rect}\left(\frac{t}{T_{obs}}\right) \text{rect}\left(\frac{f - f_0}{B}\right)$ represents the signal

support, f_0 represents the carrier frequency, z is the vector that locates a generic scatterer position, B is the transmitted signal bandwidth, T_{obs} is the observation time, $R_0(t)$ is the modulus of vector $\mathbf{R}_0(t)$, which locates the position of focusing point O , $\mathbf{i}_{R_0}(t)$ the unit vector of $\mathbf{R}_0(t)$, V is the spatial domain where the scattering matrix

$$\mathbf{z}(z) = \begin{bmatrix} \mathbf{z}^{HH}(z) & \mathbf{z}^{HV}(z) \\ \mathbf{z}^{VH}(z) & \mathbf{z}^{VV}(z) \end{bmatrix} \text{ is defined and}$$

$$\mathbf{N}(f, t) = \begin{bmatrix} N_R^{HH}(f, t) & N_R^{HV}(f, t) \\ N_R^{VH}(f, t) & N_R^{VV}(f, t) \end{bmatrix} \text{ is the polarimetric ma-}$$

trix containing the noise. The function $\text{rect}(x)$ is equal to 1 for $|x| < 0.5$, 0 otherwise.

Before proceeding, it is convenient to use a different notation, as detailed in [6], and exploit the characteristic of isotropic media that are encountered in ISAR applications. Therefore, the polarimetric data that represents the received signal can be written as follows:

$$\mathbf{S}_R = \frac{1}{\sqrt{2}} \left[S_R^{VV} + S_R^{HH}, S_R^{VH} - S_R^{HV}, 2 S_R^{HV} \right]^T \quad (2)$$

where the received signal support (f, t) has been omitted for notation simplicity.

Therefore, the received signal can be seen as a vector in the three-dimensional polarimetric space. It is worth noting that all possible projections can be obtained by means of an internal product between the received signal vector and a generic polarisation vector \mathbf{p} :

$$S_R^{(p)} = \mathbf{S}_R \cdot \mathbf{p}$$

where

$$\mathbf{p} = \frac{1}{\sqrt{2}} [p^{HH} + p^{VV}, p^{HH} - p^{VV}, p^{HV}] = |\mathbf{p}| \mathbf{w} \quad (3a)$$

$$\mathbf{w} = \begin{bmatrix} \cos \mathbf{a} \exp(j\mathbf{j}) \\ \sin \mathbf{a} \cos \mathbf{b} \exp(j\mathbf{d}) \\ \sin \mathbf{a} \sin \mathbf{b} \exp(j\mathbf{g}) \end{bmatrix} \quad (3b)$$

- \mathbf{a} is the scatterer's internal degree of freedom, which ranges in the interval $[0, 90]$ degrees [3]. The meaning of such an angle is related to the scattering properties of the target, e.g. for an ideal dipole the value of \mathbf{a} is equal to 45° . A graphical interpretation of such an angle is given in fig. 1.
- \mathbf{b} represents a physical rotation of the scatterer on the plane perpendicular to the e.m. wave propagation direction.
- $\mathbf{j}, \mathbf{d}, \mathbf{g}$ are the scatterer phases of the three polarimetric components.

Anisotropic Surfaces		Anisotropic Dihedrals	
$\mathbf{a} = 0$	$\mathbf{a} = 45$	$\mathbf{a} = 90$	
Isotropic Surface	Dipole	Isotropic Dihedral Helix	
$\begin{bmatrix} 1 & 0 \\ 0 & 1 \end{bmatrix}$	$\begin{bmatrix} 1 & 0 \\ 0 & 0 \end{bmatrix}$	$\begin{bmatrix} 1 & 0 \\ 0 & -1 \end{bmatrix}$	

Fig. 1 – Interpretation of the internal degree of freedom \mathbf{a}

It is worth noting that such a representation is meant to highlight the physical properties of the scattering mechanism induced by a given scatterer. Therefore, by defining the unit vector \mathbf{w} , it is possible to define a specific polarisation that resonates with a scatterer with given physical properties.

The same decomposition applies for the target scattering matrix. Therefore, the scattering vector obtained from the scattering matrix is

$$\mathbf{z}(\mathbf{z}) = [\mathbf{z}^{VV}(\mathbf{z}) + \mathbf{z}^{HH}(\mathbf{z}), \mathbf{z}^{VV}(\mathbf{z}) - \mathbf{z}^{HH}(\mathbf{z}), 2\mathbf{z}^{HV}(\mathbf{z})].$$

One advantage that comes out from the use of polarimetric radar is the Signal to Noise Ratio (SNR) maximisation in the polarisation space. Such an insight has been largely applied in polarimetric radar for increasing detection performance [1].

The concept of increasing the performance by finding an optimal polarisation can be extended to the ISAR image focusing problem. In other words, it can be assumed that for a particular polarimetric unit vector \mathbf{w}_{opt} the image focus reaches its maximum. This insight can be justified by considering that the image focus quality strongly depends on the time invariance of the scatterer contributions. The Doppler components for each scatterer are generally modulated by several causes. Among all the causes, including target-radar dynamics, some are related to the modulation induced by the scatterer scintillation and to the effect of noise. Both these causes can be reduced by exploiting full polarisation information. In fact, both the SNR and the modulation effect induced by the scatterer when illuminated from different point

of view can be jointly improved by finding the optimal polarisation unit vector \mathbf{w}_{opt} . The definition of such optimality criterion will be defined in section 3.

2.2 Image Formation

The process of defining the steps that lead to the image formation will be carried out without including the noise contribution as a standard way of proceeding in SAR/ISAR processing. The noise contribution will be added subsequently for SNR analysis. Motion compensation consists of removing the phase term $e^{-j\frac{4\mathbf{p}f}{c}R_0(t)}$ due to the radial movement of the focusing point O. The received signal after perfect motion compensation can be written as follows:

$$S_{rc}(f, t) = W[f, t] \int_V \mathbf{z}(\mathbf{z}) \exp\left\{-j\frac{4\mathbf{p}f}{c}[\mathbf{z}^T \mathbf{i}_{R_0}^{(z)}(t)]\right\} d\mathbf{z} \quad (4)$$

In order to reconstruct the ISAR image we consider the simple approach of the Range-Doppler (RD) technique. The RD makes use of a two-dimensional Fourier Transform (2DFT) of the motion compensated signal $S_{rc}(f, t)$ to reconstruct the complex image in the *time lag - Doppler frequency* domain. If we consider the target model as the composition of K independent scattering centres, for any given polarisation it is possible to define a reflectivity function as

$$\mathbf{z}^{(p)}(\mathbf{z}) = \sum_{k=1}^K a_k^{(p)} \mathbf{d}(\mathbf{z} - \mathbf{z}_k^{(p)}). \text{ It is worth noting that such}$$

scatterers can be considered semi-ideal. In fact, they are interpreted as ideal in terms of being independent of each other and in terms of dimensions (point-like), but their response changes according to the polarisation used. The polarimetric complex ISAR image of a target composed of a set of semi-ideal scatterers can be written as follows:

$$\begin{aligned} I^{(p)}(\mathbf{t}, \mathbf{n}) = & FT^2 \left[W[f, t] \sum_{k=1}^K a_k^{(p)} \exp\left\{-j\frac{4\mathbf{p}f}{c}[(\mathbf{z} - \mathbf{z}_k^{(p)})^T \mathbf{i}_{R_0}^{(z)}(t)]\right\} \right] \\ = & T_{obs} B \sum_{k=1}^K a_k^{(p)} \text{sinc}\left[T_{obs}(\mathbf{n} - \mathbf{n}_k^{(p)})\right] \cdot \\ & \cdot \text{sinc}\left[B(\mathbf{t} - \mathbf{t}_k^{(p)})\right] \exp\left\{-j2\mathbf{p}f_0(\mathbf{t} - \mathbf{t}_k^{(p)})\right\} \end{aligned} \quad (5)$$

where $a_k^{(p)}$ is the complex amplitude of the k -th scatterer relative to the generic polarisation \mathbf{p} , $\mathbf{d}(\mathbf{z} - \mathbf{z}_k^{(p)})$ is the Dirac function centred at the position of the k -th scatterer and \mathbf{n}_k and \mathbf{t}_k represent the coordinates of the scatterers on the image plane in the *time lag - Doppler frequency* domain. It is worth noting that the polarisation affects both the scatterer amplitude and the scatterer position. This latter point has been taken into account because in the real world the scattering centre position is determined by a weighted sum of several contributions. Because such weights depend on the polarisation, the scattering centre location also depends on it. It is worth noting that the polarimetric complex ISAR image of a set of semi-ideal scatterers is still composed of a sum of

sinc-like shaped terms (see eq. (3)), as it was in the case of signal polarisation ISAR.

3. OPTIMAL POLARIMETRIC ISAR IMAGE AUTOFOCUSING

Before defining an algorithm for optimal autofocusing of ISAR polarimetric images, it is worth noting that point O on the target is an arbitrary point because its location on the target does not affect the image focus (a demonstration is given in [5]). Moreover, its position depends on the specific polarisation that is used.

The phase term to be removed from the received signal can be written as $e^{-j\frac{4pf}{c}R_0^{(p)}(t)}$.

In this paper an algorithm, namely the Image Contrast Based Technique (ICBT), already used for single polarisation ISAR image autofocusing will be considered and extended to the case of fully polarimetric ISAR. The ICBT maximises the contrast of the ISAR image. Such an optimisation problem can be solved in a wider domain that includes the original space with the polarimetric space adjoined.

The new optimisation problem can be formalised for the ICBT by defining a new cost function with support in its original space \mathbf{x} extended to the union of it with the space of the polarimetric vector. Therefore, in formula:

$$(\hat{\mathbf{x}}, \hat{\mathbf{p}}) = \operatorname{argmax}_{\mathbf{x}, \mathbf{p}} \{IC(\mathbf{x}, \mathbf{p})\} \quad (6)$$

where $IC(\mathbf{x}, \mathbf{p})$ is the new image contrast function defined for the polarimetric data.

The optimisation problem of eq. (6) can be solved in several ways. In the scalar implementation of the ICBT, two solutions were provided in [5], [7]. The first solution was based on the use of the Nelder-Mead algorithm and the second was based on the use of genetic algorithms. In this paper only the first solution will be used. When the Nelder-Mead approach is followed, a second order polynomial model is used and an initial guess of the parameters to be estimated must be provided. In [5] a solution for rough estimation of target radial velocity and acceleration was provided. In order to proceed with the application of the ICBT to the fully polarimetric ISAR data, a solution for the initial polarisation vector must also be provided. The problem can be solved by means of the following algorithm:

1. The polarisation vector that provides the maximum SNR is obtained by solving the optimisation problem of eq. (7).

$$\hat{\mathbf{p}}_M = \operatorname{argmax}_p \left\{ \frac{\iint |S_R^{(p)}(f, t)|^2}{\iint |N_R^{(p)}(f, t)|^2} \right\} \quad (7)$$

It is worth noting that the SNR can be assumed maximum when the signal energy reaches its maximum, provided that the noise level is the same in all the polarisation channels (basically when the noise level in the H and V receiving channels is the same). Therefore, eq. (7) can be simplified as follows:

$$\hat{\mathbf{p}}_M \equiv \operatorname{argmax}_p \left\{ \iint |S_R^{(p)}(f, t)|^2 \right\} \quad (8)$$

2. An initial guess for the values (α_1, α_2) , namely the target radial velocity and acceleration can be obtained by applying the Radon Transform for the radial velocity and by running a one-dimensional optimisation problem for the radial acceleration (see [5]). The scalar problem of finding the initial guess for the values (α_1, α_2) is applied to the received signal with polarisation $\hat{\mathbf{p}}_M$ as found at step 1;

$$(\hat{\mathbf{a}}_1^{(\hat{\mathbf{p}}_M)}, \hat{\mathbf{a}}_2^{(\hat{\mathbf{p}}_M)}) = \operatorname{argmax}_{\mathbf{a}_1, \mathbf{a}_2} \{IC^{(\hat{\mathbf{p}}_M)}(\mathbf{a}_1, \mathbf{a}_2)\} \quad (9)$$

where the image contrast (IC) is defined as follows:

$$IC^{(\hat{\mathbf{p}}_M)}(\mathbf{a}_1, \mathbf{a}_2) = \frac{\sqrt{A \left\{ \left[I^{(\hat{\mathbf{p}}_M)}(\mathbf{t}, \mathbf{n}; \mathbf{a}_1, \mathbf{a}_2) - A \{ I^{(\hat{\mathbf{p}}_M)}(\mathbf{t}, \mathbf{n}; \mathbf{a}_1, \mathbf{a}_2) \} \right]^2 \right\}}}{A \{ I^{(\hat{\mathbf{p}}_M)}(\mathbf{t}, \mathbf{n}; \mathbf{a}_1, \mathbf{a}_2) \}}$$

3. The focusing parameters together with the optimal polarisation parameters are jointly estimated by maximising the IC. Analytically, this can be expressed as follows:

$$(\hat{\mathbf{a}}_1, \hat{\mathbf{a}}_2, \hat{\mathbf{p}}) = \operatorname{argmax}_{\mathbf{a}_1, \mathbf{a}_2, \mathbf{p}} \{IC^{(p)}(\mathbf{a}_1, \mathbf{a}_2)\}$$

where

$$IC^{(p)}(\mathbf{a}_1, \mathbf{a}_2) = \frac{\sqrt{A \left\{ \left[I^{(p)}(\mathbf{t}, \mathbf{n}; \mathbf{a}_1, \mathbf{a}_2) - A \{ I^{(p)}(\mathbf{t}, \mathbf{n}; \mathbf{a}_1, \mathbf{a}_2) \} \right]^2 \right\}}}{A \{ I^{(p)}(\mathbf{t}, \mathbf{n}; \mathbf{a}_1, \mathbf{a}_2) \}}$$

with the initial guess $(\hat{\mathbf{a}}_1^{(\hat{\mathbf{p}}_M)}, \hat{\mathbf{a}}_2^{(\hat{\mathbf{p}}_M)}, \hat{\mathbf{p}}_M)$.

For the sake of clarity, the proposed algorithm is summarised in fig. 2.

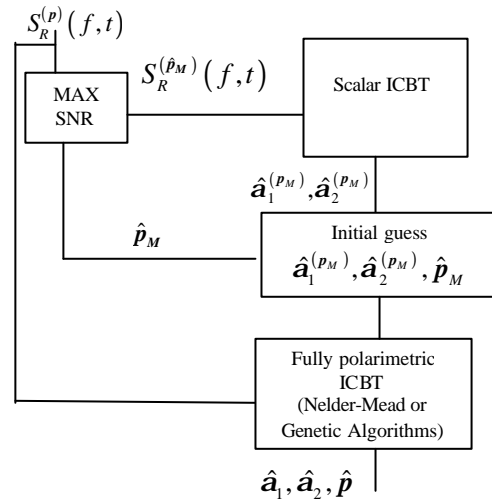


Fig. 2 – Algorithm block diagram

4. SIMULATION RESULTS

In order to prove the effectiveness of the proposed technique for polarimetric ISAR image autofocusing, a simulation approach is followed. The generation of a fully polarimetric radar received signal cannot be accomplished by simply using a set of ideal scatterers. In fact, an ideal scatterer

would backscatter the signal in the same way regardless of the polarisation used. Real continuous targets respond accordingly to the polarisation used. In general, the performance of a radar depends on the polarisation used because a given target may be more sensitive to a polarisation rather than another. This concept can be extended to the case of radar imaging performance. Image quality indicators, such as image contrast, image entropy, image peak and visual quality can be affected by the polarisation. Therefore, the generation of the signal must take into account the scattering mechanisms that occur on the target and that are affected by the polarisation used. The signal generator represents a key point for the algorithm performance analysis because it must produce a realistic signal as close as possible to a real polarimetric signal. For this purposes, an electromagnetic toolbox, namely the “EMvironment” has been used for our purposes. Details about Environment can be found in [8].

4.1 Signal generation

In this simulation it is assumed that the ship target is illuminated by an airborne radar, as indicated in fig.3. In such a scenario, the radar-target dynamics are affected by the radar rectilinear motion, the ship rectilinear motion and the ship angular motions induced by the sea surface. It must be mentioned that it is not the aim of this work to show how dedicated ISAR processing can solve problems related to radar-target dynamics, such as fast manoeuvring targets in ISAR imaging of airplanes or sea surface induced angular motions in ISAR imaging of ships. Solutions of such problems in single polarisation mode have been proposed in [9], [10], [11]. Therefore, a simple ISAR scenario where the radar-target dynamics are generated by only the airplane and ship rectilinear motion has been considered. The geometry of the simulation is shown in fig. 3, whereas in fig. 4 a picture of the ship model is provided. The parameters of the simulations are shown in table I

4.2 Results

A comparison of the ISAR images that are obtained by using single channel ISAR processing and fully polarimetric ISAR processing are shown in fig. 5-9. Fig. 5, 6 and 7 show the ISAR image that are obtained by processing the VV, HH and VH channels separately. It is quite evident that the three channels show quite different details of the target. The maximisation of the SNR in the polarimetric space provides a particular polarisation which is the linear combination of the four polarimetric channels that produces the maximum SNR. The ISAR image that is produced by processing such a signal is shown in fig. 8 The evident characteristic that distinguishes the ISAR image in fig. 8 from the previous ones is the higher energy content as highlighted by the image intensity grey scale. Nevertheless, the results in terms of image focusing do not change significantly. In fact it is hard to decide whether the ISAR image in fig. 8 is more focussed than the ISAR image in fig. 5 and 6 (VV and HH polarisation). In fig. 9 the ISAR image obtained by running the proposed algorithm is shown. The high focus of the image is quite evident if compared with the other ISAR images. The structures on the ship, especially the posts, are distinguishable in the

ISAR image. It is worth noting that the peak value is lower than in the case of fig. 8. In fact, as discussed throughout the paper, a higher SNR does not necessarily produce a better focussed image. The values of the image contrast for each ISAR image are shown in table II. As expected, the ISAR image produced with the proposed algorithm provides the largest contrast. Moreover, it is interesting to analyse the polarisations that maximise the SNR and the IC, which are shown in table III. The main scattering mechanism in both the cases is dominated by an almost Isotropic Dihedral characteristic ($\alpha \approx 80^\circ$). It is also worth noting that geometrical orientation of the ship structures makes the difference between the two cases.

Table I – Simulation parameters

Parameter	Value
Minimum frequency	1 GHz
Frequency step	1.6 MHz
Bandwidth	100.8 MHz
PRF	100 Hz
Ideal range resolution	1.49 m
Ideal cross-range resolution	1.36 m
Ship velocity	30 Km/h
Ship size	18 x 6 x 2 m

Table II – Image Contrast

VV	HH	HV	SNR	MAX POL
2.71	2.73	2.53	2.54	3.65

Table III - Polarimetric parameters

Parameter	MAX SNR (degrees)	MAX IC (degrees)
α	81	79
β	62	42
γ	128	296
δ	133	231
ϵ	312	~ 0

5. CONCLUSIONS

In this paper, a framework for polarimetric multichannel ISAR processing has been provided. Moreover, a novel auto-focusing technique for polarimetric ISAR data has been proposed. Results demonstrate that the use of fully polarimetric radar produces better image autofocusing.

ACKNOWLEDGEMENT

The authors would like to thank Prof. A. Monorchio for the use of the software *EMvironment*. Special thanks also go to A. Corucci and A. Menegato for their useful help with the simulations.

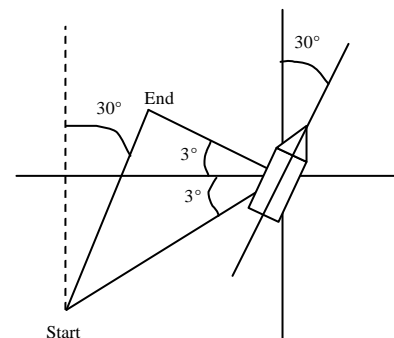


Fig. 3 – Simulation geometry

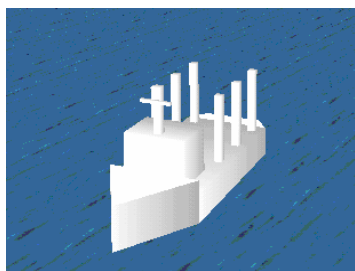


Fig. 4 – Ship model

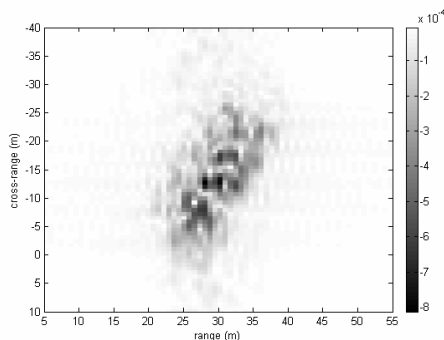


Fig. 5 – VV pol ISAR image

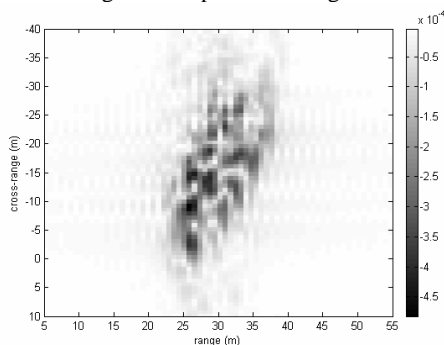


Fig. 6 – HH pol ISAR image

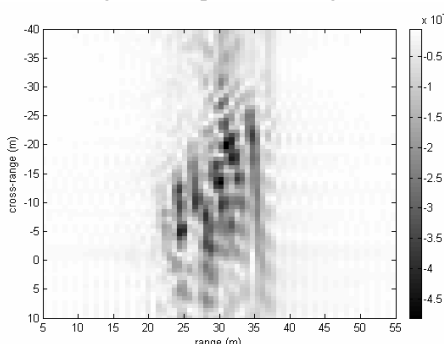


Fig. 7 – VH pol ISAR image

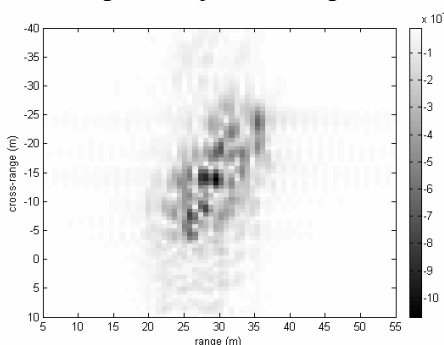


Fig. 8 – max_SNR ISAR image

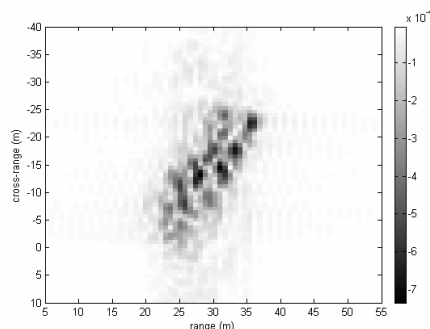


Fig. 9 – max pol ISAR image

REFERENCES

- [1] L. M. Novak, M. B. Sechtin, M. J. Cardullo, "Studies of target detection algorithms that use polarimetric radar data", *IEEE Transactions on Aerospace and Electronic Systems*, Volume 25, Issue 2, pp. 150 – 165, Mar. 1989.
- [2] J. J. van Zyl, "Unsupervised classification of scattering behaviour using radar polarimetry data", *IEEE Transactions on Geoscience and Remote Sensing*, Volume 27, Issue 1, pp. 36 – 45, Jan. 1989.
- [3] S.R. Cloude, K.P. Papathanassiou, "Polarimetric SAR Interferometry", *IEEE Tr. on Geoscience and Remote Sensing*, Vol. 36, Issue 5, Part 1, Sept. 1998, Page(s):1551 - 1565.
- [4] G. Wang, X-G Xia, V.C. Chen, "Radar imaging of moving targets in foliage using multifrequency multiaperture polarimetric SAR", *IEEE Tr. on Geoscience and Remote Sensing*, Vol. 41, Issue 8, Aug. 2003, Page(s):1755 - 1764
- [5] M. Martorella, F. Berizzi, B. Haywood, "A Contrast Maximization Based Technique for 2D ISAR Autofocusing", *IEE Proceedings on Radar Sonar and Navigation*, Volume 152, Issue 4, pp. 253 – 262, Aug. 2005.
- [6] S. R. Cloude, E. Pottier, "A review of target decomposition theorems in radar polarimetry", *IEEE Transactions on Geoscience and Remote Sensing*, Volume 34, Issue 2, pp. 498 – 518, Mar. 1996.
- [7] M. Martorella, F. Berizzi, S. Bruscoli, "Use of Genetic Algorithms for Contrast Maximization and Entropy Minimization in ISAR Autofocusing", to appear on *Journal of Applied Signal Processing - Special Issue on Inverse Synthetic Aperture Radar*, in Apr. 2006.
- [8] "EMvironment 2.1. User Guide", Microwave and Radiation Lab, Dept. of "Ingegneria dell'Informazione", University of Pisa, 2006.
- [9] S. Qian and D. Chen, *Joint Time-Frequency Analysis: Method and Application*, Chapter 8, Prentice Hall, 1996.
- [10] F. Berizzi, E. Dalle Mese, M. Diani, M. Martorella, "High resolution ISAR imaging of maneuvering targets by means of the Range Instantaneous Doppler technique: modeling and performance analysis", *IEEE Transactions on Image Processing*, Volume: 10, No. 12, pp 1880 –1890, Dec. 2001.
- [11] M.Martorella, F.Berizzi, "Time Windowing for Highly Focussed ISAR Image Reconstruction", *IEEE Transactions on Aerospace and Electronic Systems*, Volume 41, Issue 3, pp. 992 - 1007, Oct. 2005.